Supporting Information

Transmembrane Ion Channels Formed by a Star of David [2]Catenane and a Molecular Pentafoil Knot

David P. August,[†] Stefan Borsley,[†] Scott L. Cockroft,[§] Flavio della Sala,[†‡] David A. Leigh*[†] and Simon J. Webb[†‡]

† Department of Chemistry, University of Manchester, Oxford Road, Manchester M13 9PL, United Kingdom

‡ Manchester Institute of Biotechnology, University of Manchester, 131 Princess Street, Manchester M1 7DN, United Kingdom

§ EaStCHEM School of Chemistry, University of Edinburgh, Joseph Black Building, David Brewster Road, Edinburgh EH9 3FJ, United Kingdom

Contents

S1. General experimental procedures

Unless stated otherwise, reagents were obtained from commercial sources and used without purification. All chemicals, reagents, salts, buffers, cholesterol and egg yolk phosphatidylcholine (EYPC) lipid were purchased from Sigma Aldrich, UK. 1,2-diphytanoyl-*sn*-glycero-3-phosphocholine was purchased form Avanti Polar Lipids. Deionized water for vesicle experiments was obtained by a milli-Q water purifier (Millipore). HPLC grade water from Fischer UK was used for single-channel recordings. Anhydrous solvents were obtained by passing the solvent through an activated alumina column on a Phoenix SDS (solvent drying system; JC Meyer Solvent Systems, CA, USA). Compounds **1**–**6** were synthesised as previously reported, and all spectral data matched the previously reported data.[S1–S3] ^{1}H NMR spectra were recorded on a Bruker Avance III instrument with an Oxford AS600 magnet equipped with a cryoprobe [5 mm CPDCH ^{13}C-^{1}H/D] (600 MHz) at a constant temperature of 20 °C and processed using MestReNova 11.0. ^{1}H and ^{13}C chemical shifts are reported in parts per million (ppm) from low to high field and referenced to the literature values for chemical shifts of residual non-deuterated solvent, with respect to tetramethylsilane (0.00 ppm) as an external standard. Standard abbreviations indicating multiplicity are used as follows: bs (broad singlet), d (doublet), dd (doublet of doublets), m (multiplet), q (quartet), s (singlet), t (triplet), tt (triplet of triplets), J (coupling constant – quoted in Hz). Fully characterized compounds were chromatographically homogeneous. Flash column chromatography was carried out using Silica 60 Å (particle size 40–63 μm, Sigma Aldrich, UK) as the stationary phase. Size exclusion chromatography was carried out using Bio-Beads S-X3 support beads as the stationary phase. TLC was performed on precoated silica gel plates (0.25 mm thick, 60 F254, Merck, Germany) and visualized using both short and long wave ultraviolet light in combination with standard laboratory stains (basic potassium permanganate, acidic ammonium molybdate and ninhydrin). Low resolution ESI mass spectrometry was performed with a Thermo Scientific LCQ Fleet Ion Trap Mass Spectrometer or an Agilent Technologies 1200 LC system with an Advion Expression LCMS single quadrupole MS detector. High-resolution mass spectrometry (HRMS) was carried out at the Mass Spectrometry Service, School of Chemistry, University of Manchester. Fluorescence measurements were performed on a Varian Cary Eclipse Fluorescence spectrophotometer equipped with a thermostatted cell holder with a stirring function. All fluorescence experiments were conducted at 293 K and with maximum stirring. UV-vis measurements were performed on a Jasco EHC-716 UV-vis spectrophotometer in quartz cuvettes (path length = 10 mm). Molecular modelling and viewing/modification of crystal structures was performed in Spartan ’14 and Biovia Discovery Studio Visualizer ’19.

S2. Structural analysis of compounds

S2.1 Synthesis and characterization

All compounds were synthesised in accordance with literature procedures and structural characterization data was in agreement with reported values.

Compound **1** was synthesized in accordance with reference S1.

Compound **2** was synthesized in accordance with reference S1.

Compound **3** was synthesized in accordance with reference S2.

Compound **4** was synthesized in accordance with reference S2.

Compound **5** was synthesized in accordance with reference S3.

Compound **6** was synthesized in accordance with reference S2.

S2.2 Analysis of crystal structures of knots and links

X-Ray crystal structures of compounds **2**[S1] and **3**[S2] were published in references S1 and S2 respectively. The crystal structure of compound **2** contains a Cl^- anion bound in the central cavity while the crystal structure of **3** contains a hexafluorophosphate anion bound within the central cavity.

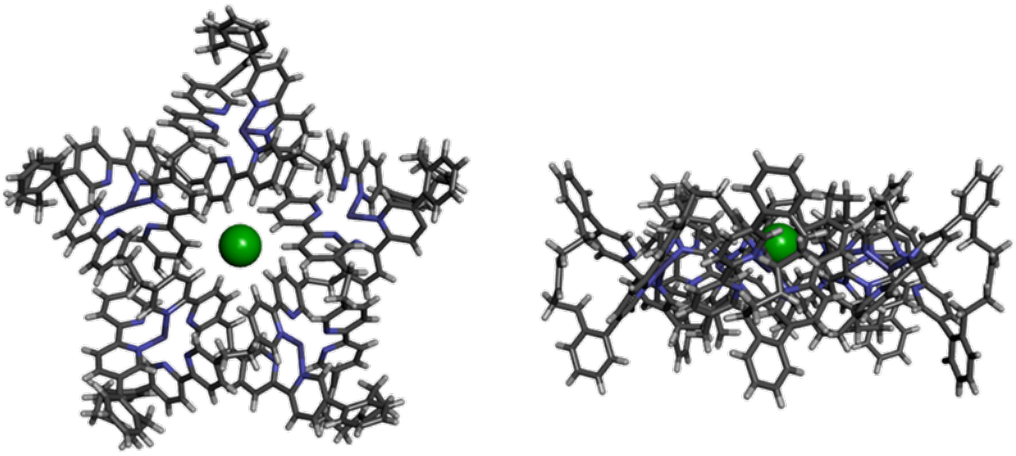

Figure S1 X-Ray crystal structures of pentafoil knot **2**[S1] showing the central bound chloride anion. Hexafluorophosphate anions and solvent removed for clarity. Carbon coloured dark grey, iron coloured black, nitrogen blue, hydrogen white, chloride green.

The crystal structures were overlaid with a solvent accessible isosurface using a 1.4 Å probe radius in BIONOVA Discovery Studio Visualizer v19 software.

The cavity diameters were determined by measuring the minimum H-H distance across the middle of the cavity. 2 Å was subtracted from this value to account for a typical ^{1}H radius (1 Å).

S2.3 Calculated structures

Compound 6

Compound **6** was computationally modelled (Spartan 16.0) by substituting the appropriate groups then computationally minimizing the crystal structure of compound **3**. The geometry of compound **6** was minimized by molecular mechanics (MMFF). The rigid core of the molecule remained in an almost identical geometry, albeit with a more disordered ligand exterior, to that of compound **3**.

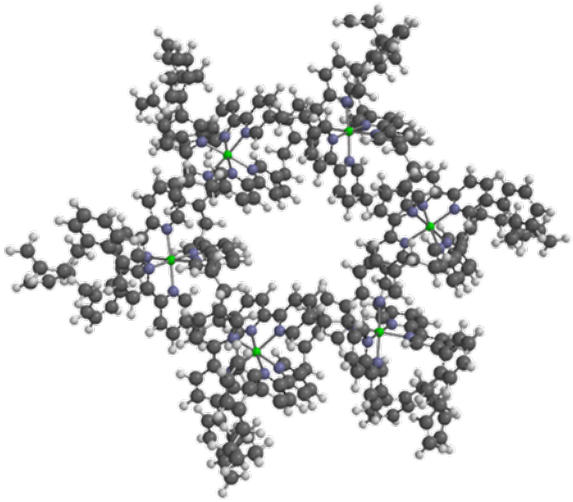

Figure S2 Minimized (MMFF) modelled structure of circular helicate **6** showing a similar cavity to Star of David catenane **3**, but a more disordered ligand exterior.

Compound 3

A single-point energy calculation allowed determination of the electrostatic potential surface of compound **3**. Starting from the crystal structure of compound **3**, a molecular mechanics (MMFF) geometry minimization made minor changes to the structure. Subsequently, the electrostatic potential surface was calculated (Hartree-Fock STO-3G).

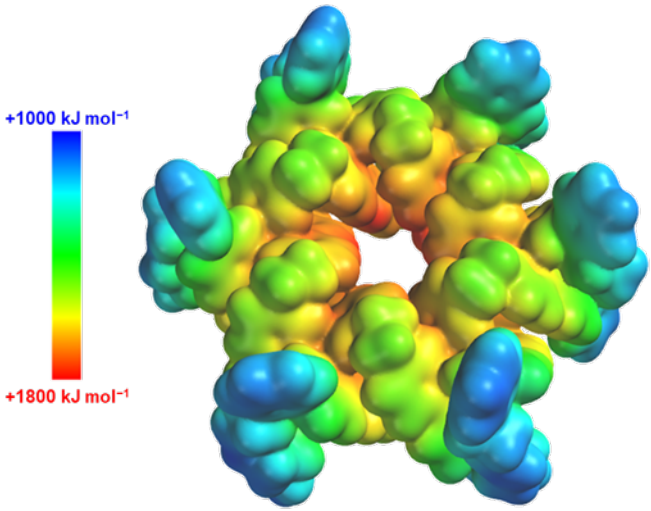

Figure S3 Electrostatic potential surface of Star of David catenane **3** (Hartree-Fock STO-3G) showing the highly positive central cavity and the more lipophilic edges.

S2.4 Partitioning of 2 and 3 between water and 1-octanol

To mimic the partitioning of pentafoil knot **2** and Star of David link **3** between the aqueous phase and the phospholipid bilayer, an attempt was made to determine the logP values for **2** and **3**.

Briefly, a 1 mM solution of pentafoil knot **2** or Star of David link **3** (50 μL, in MeCN) was added to the octanol (top) phase of a biphasic mixture of octanol and milliQ water (10 mL, 1:1 *v/v,* to give 5 μM across the total volume of both phases) (Figure S4a). However after the phases had been vigorously shaken, some precipitation was observed (Figure S4b). Nonetheless a significant amount of the pentafoil knot **2** or Star of David link **3** was still dissolved in the upper organic layer, with no visible dissolution in the lower aqueous phase. The presence of coloured insoluble material in the aqueous phase prevented quantitative determination of logP for either compound, although this value would appear to be substantial and similar for both.

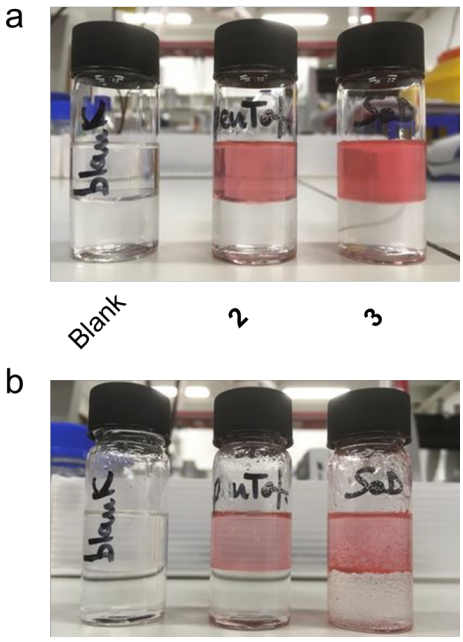

Figure S4 (a) Partitioning of pentafoil knot **2** and Star of David link **3** between 1-octanol and water. (b) After shaking, some precipitation of both complexes was observed.

S3. Vesicle studies

S3.1 HPTS assays

Preparation of large unilamellar vesicles for HPTS assays

Egg yolk phosphatidylcholine (EYPC, 49 mg, 64 μmol) and cholesterol (6 mg, 16 μmol) were dissolved in 2 mL chloroform (spectroscopic grade) in a 10 mL round-bottom flask. The solvent was removed under reduced pressure, resulting in a thin film of lipid on the inside wall of the round-bottom flask, which was dried further under high vacuum for 16 hours. Trisodium 8-hydroxypyrene-1,3,6-trisulfonate (HPTS, 100 mM) was dissolved in buffer (20 mM 3-(*N*-morpholino) propanesulfonic acid (MOPS), 100 mM MX (M = Li, K, Na, Rb or Cs and X = F, Cl, Br, I, SCN or NO_3) adjusted to pH 7.4 using NaOH). The HPTS buffer solution (1.2 mL) was added to the lipid film. The mixture was subjected to vortex mixing until the film had completely detached from the sides of the flask. The resulting lipid suspension was gently warmed and extruded 19 times through a 200 nm polycarbonate membrane in an Avestin Liposofast extruder to give a suspension of 200 nm large unilamellar vesicles.

Unencapsulated HPTS dye was removed by gel permeation chromatography (GPC) on PD-10 SEC columns (Sephadex G-25). An aliquot of the vesicle suspension (1 mL) was added to a column that had been equilibrated with the appropriate buffer (the same buffer as used for vesicle preparation, but without added HPTS). Once the vesicle solution had run onto the GPC column, further buffer (1.5 mL) was added and allowed to run onto the GPC column. A further solution of buffer (3.5 mL) was added to elute the vesicles, which were collected to give a vesicle stock solution (3.5 mL, final concentration of phospholipid = 15.2 mM, final concentration of cholesterol = 3.8 mM). Two green bands were visible on the column, indicating successful separation of the HPTS-loaded vesicles (faster band) from unencapsulated HPTS (slower band).

Procedure for HPTS assays

The vesicle stock solution (100 μL) was diluted with buffer (1.9 mL, same buffer as in the vesicles) to give a final volume of 2 mL (final phospholipid concentration 0.76 mM, final cholesterol concentration 0.19 mM). The vesicle suspension was added to a fluorescence cuvette equipped with a stirrer bar. The ionophoric compound (5 μL of a 1 mM solution in MeCN, final concentration = 2.5 μM, 0.26 mol% relative to total EYPC/cholesterol) was added at time 0 mins and the fluorescence emission at 510 nm was observed, resulting from the simultaneous excitation at 405 nm and 460 nm. A base pulse of 1 M NaOH (aq.) (13 μL) was added after 1 minute. Finally, Triton X-100 detergent in MOPS buffer (20 μL, 10% *v*/*v* solution) was added after 6 minutes to lyse the vesicles. Data was collected for a further 2 minutes to ensure the vesicles were completely lysed.

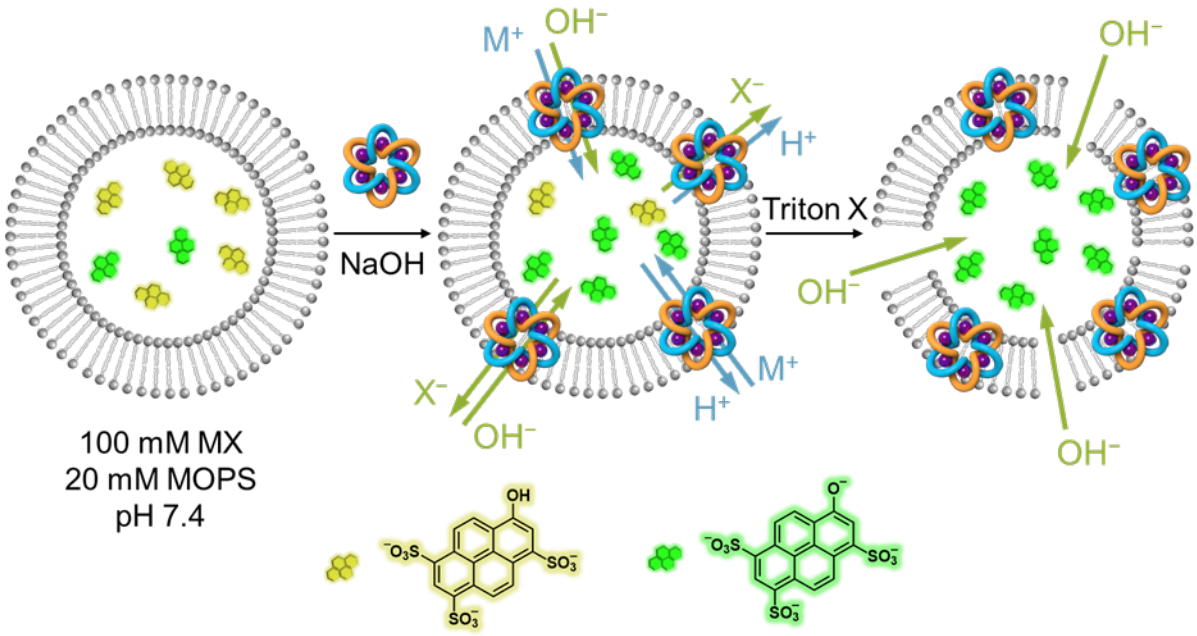

Figure S5 Schematic representation of HPTS assays. The fluorescence emission arising from the protonated (shown yellow) and deprotonated (shown green) forms of HPTS is observed. Internal pH change can occur through any combination of antiport (M^+/H^+, X^-/OH^-) or symport (M^+/OH^-, X^-/H^+), as shown. Excitation at 405 nm results in emission at 510 nm which decreases as pH increases. Excitation at 450 nm results in emission at 510 nm which increases as pH increases.

Data processing for HPTS assays

The fluorescence emission 510 nm resulting from excitation at 405 nm was divided by the emission at 510 nm resulting from excitation at 460 nm to give a fluorescence ratio. Data from time courses were normalized from 0% to 100% according to equation S1, with 0% corresponding to the fluorescence ratio prior to base pulse addition, and 100% corresponding to the fluorescence after addition of Triton X-100 and complete lysing of the vesicles.

$$I_{norm} = (F_t - F_0) / (F_\infty - F_0) \qquad \textbf{equation S1}$$

Where I_{norm} is the normalized fluorescence ratio, and F is the measured fluorescence, with $F_0 = F_t$ at addition of base pulse, $F_\infty = F_t$ at saturation after complete leakage.

Fitting HPTS assay data to pseudo first order rate equations

The normalised fluorescence data (I_{norm}) was fitted to first order kinetics using an equation of the general form:

$$I_t = I_\infty - e^{((-k_{obs} \times t) + ln(I_\infty))} \qquad \textbf{equation S2}$$

Where t = time in seconds, I_t is the normalized fluorescence ratio at time t, I_∞ is the final normalised fluorescence intensity at t = ∞ and k_{obs} is the rate constant. Data were fitted iteratively in Microsoft Excel 2016, minimising the square of the residuals between the experimental data and the fitted data.

Data were fitted from time 0 s (addition of compound) rather than time 60 s (addition of base pulse) in line with previously reported data analysis.[S4] Residuals from 90 s to 300 s were minimized and two parameters, k_{obs} and I_∞ were fitted.

All HPTS assays were repeated three times and generally showed good experimental reproducibility.

Blank HPTS assays for different salts

Blank HPTS assays were conducted in all buffers to establish a background rate of ion transport. MeCN (5 μL) was added at time 0 s. The general procedure for HPTS assays was subsequently followed. Data was fitted as described above. Where the rate was too slow to fit, a k_{obs} of <0.001 s^{-1} was assumed.

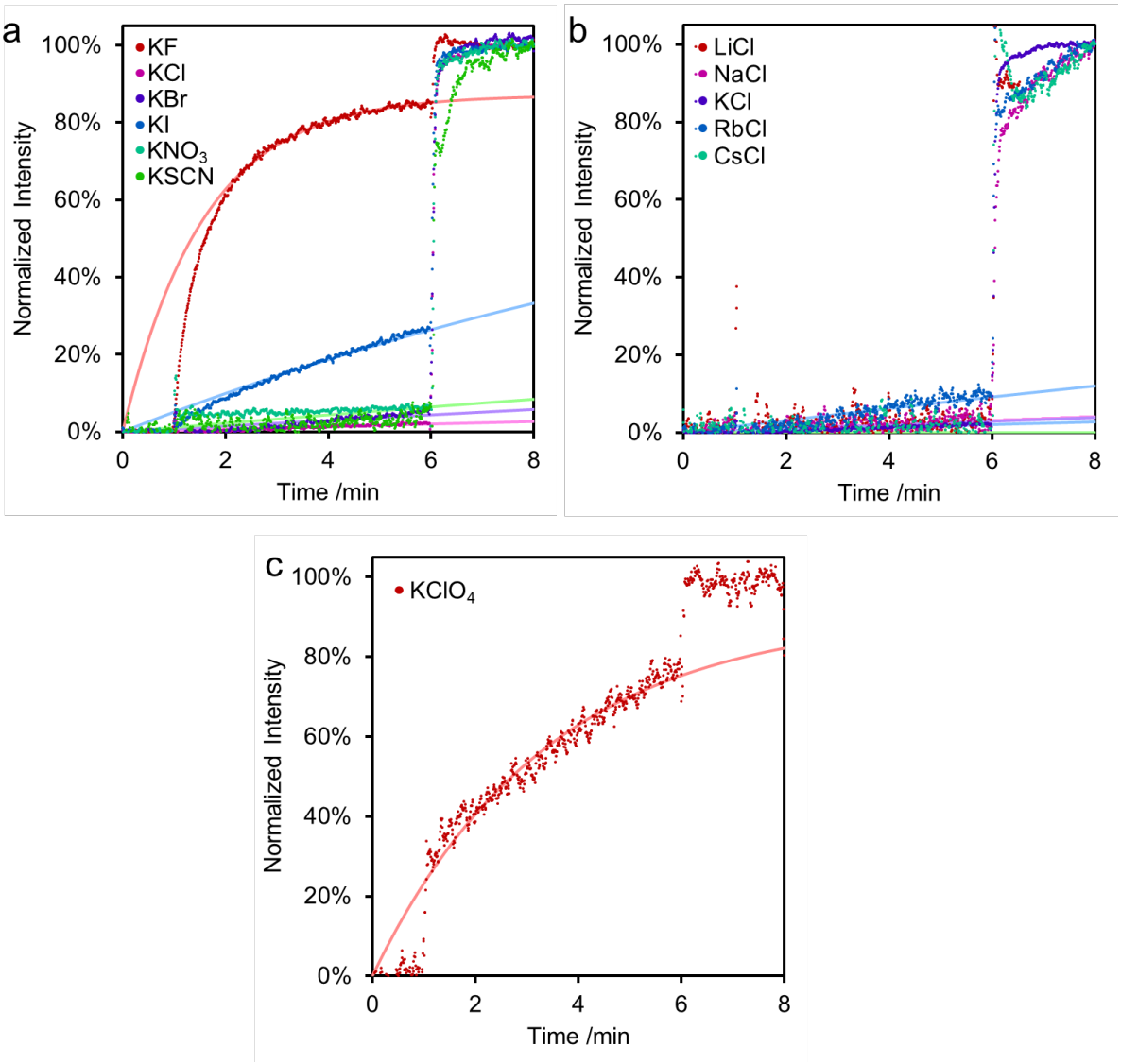

Figure S6 HPTS assays and data fitting for MeCN (5 μL) blanks with no ionophoric compound, showing the background rate of ion transport in a range of different (a) anions, (b) cations and (c) $KClO_4$ (20 mM MOPS, 100 mM MX, pH 7.4); a significant background rate was observed for this lipophilic anion. Ionophore added at 0 min, base pulse added at 1 min, Triton X-100 added at 6 mins.

Table S1 Table of the measured background rate constants for ion transport in a range of salts (20 mM MOPS, 100 mM MX, pH 7.4).

Salt	Background ion transport rate / × 10^{-3} s^{-1}
KF	11 ± 0.5
KCl	<0.1
KBr	0.15 ± 0.03
KI	1.0 ± 0.1
KSCN	<0.1
KNO_3	<0.1
$KClO_4$	4.9 ± 0.3
LiCl	<0.1
NaCl	<0.1
KCl	<0.1
RbCl	0.32 ± 0.01
CsCl	<0.1

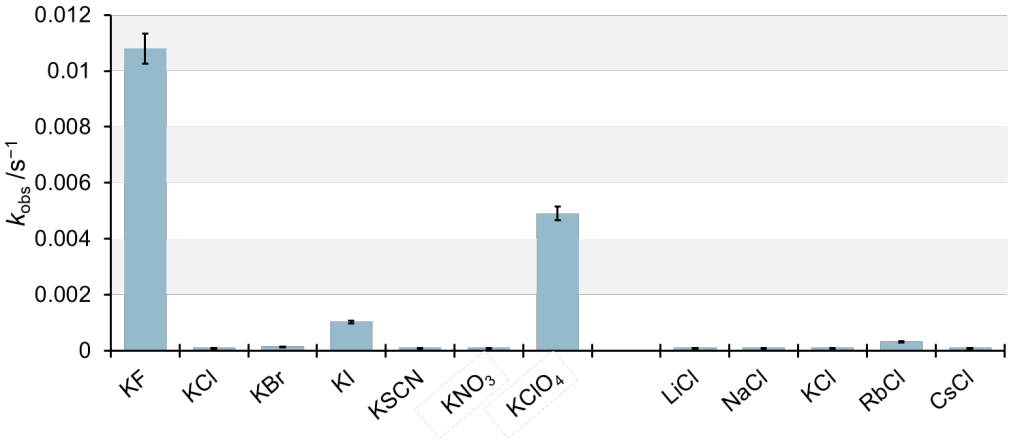

Figure S7 Observed rate constants for background ion transport in a range of salts (20 mM MOPS, 100 mM MX, pH 7.4).

HPTS assays for compounds 2, 3, 5 and $Fe^{II}(bipy)_3^{2+}$

HPTS assays were conducted as described in the general procedure. The observed rate constants for the ion transport were determined (fits as shown in Figure S7a) and the background rate from the solvent was subtracted (subtracted data shown in Figure S7b and c).

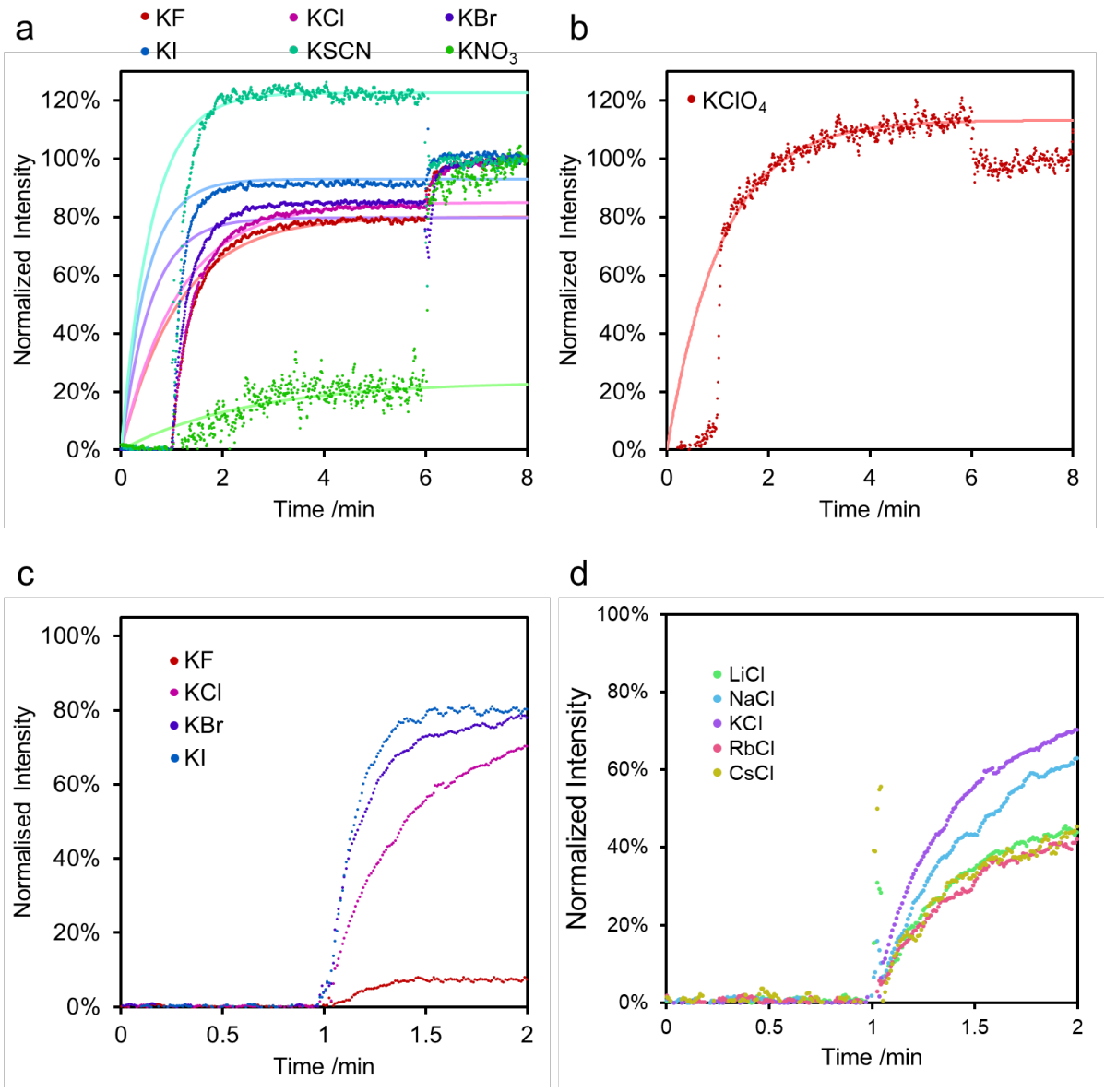

Figure S8 (a) and (b) HPTS assays and data fitting for Star of David catenane **3** (5 μL of a 1 mM solution) showing the rate of ion transport (20 mM MOPS, 100 mM MX, pH 7.4). Ionophore added at 0 min, base pulse added at 1 min, Triton X-100 added at 6 mins. (c) Background data subtracted from Star of David catenane **3** data for the anion series. (d) Background data subtracted from Star of David catenane **3** data for the cation series.

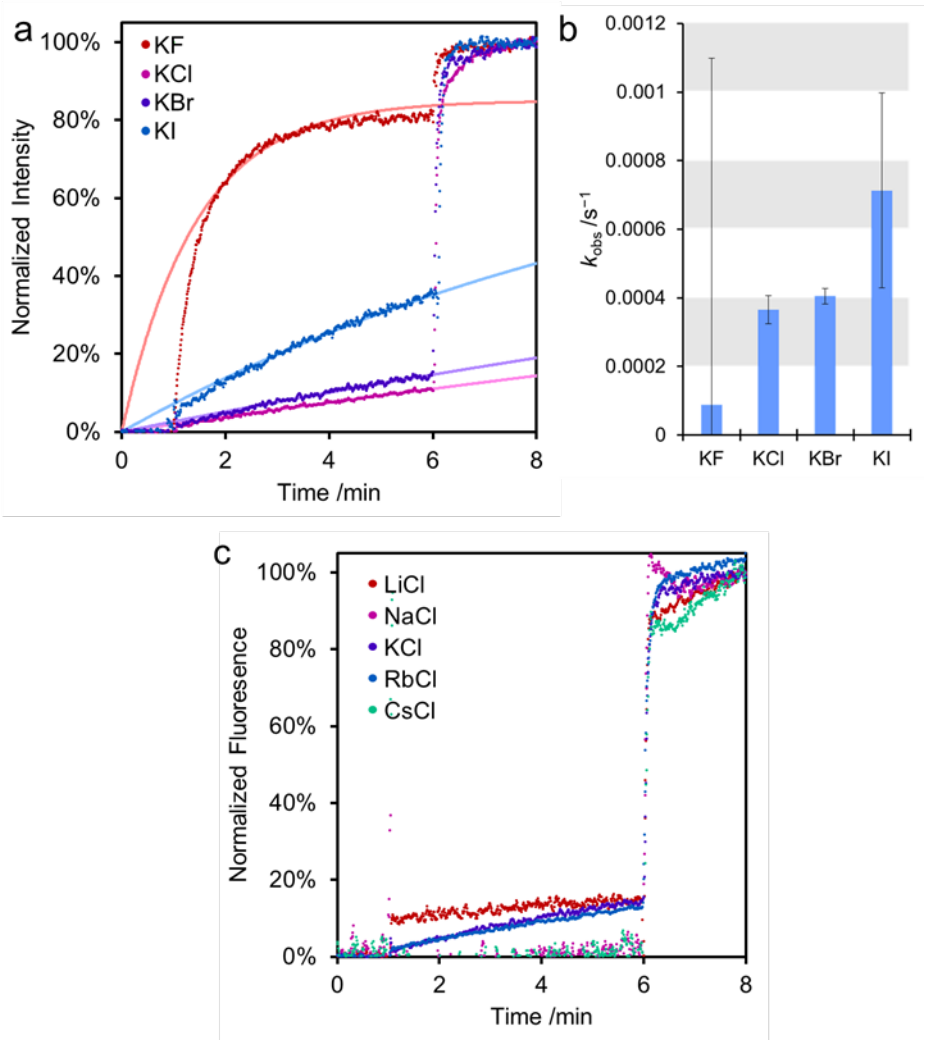

Figure S9 (a) HPTS assays and data fitting for pentafoil knot **2** (5 μL of a 1 mM solution) showing the rate of ion transport (20 mM MOPS, 100 mM MX, pH 7.4) for the halide anion series. (b) Observed rate constants for ion transport with pentafoil knot **2** subtracting the background rates from the observed rates in a range of salts (20 mM MOPS, 100 mM MX, pH 7.4). Ionophore added at 0 min, base pulse added at 1 min, Triton X-100 added at 6 mins. Fluoride error bar is large due to the high intrinsic background rate. (c) HPTS assays and data fitting for pentafoil knot **2** (5 μL of a 1 mM solution) showing the rate of ion transport (20 mM MOPS, 100 mM MX, pH 7.4) for the alkali cation series.

Table S2 Table of the measured observed rate constants for ion transport with Star of David catenane **3** and pentafoil knot **2** in a range of salts (20 mM MOPS, 100 mM MX, pH 7.4).

Salt	Star of David catenane **3** ion transport rate (observed) / × 10^{-3} s^{-1}	Pentafoil knot **2** ion transport rate (observed) / × 10^{-3} s^{-1}
KF	14.1 ± 0.1	10.8 ± 0.1
KCl	15.8 ± 0.2	0.431 ± 0.04
KBr	23.2 ± 0.5	0.552 ± 0.02
KI	31.2 ± 0.2	1.75 ± 0.03
KSCN	31.5 ± 0.5	n.d.
KNO_3	6.67 ± 0.4	n.d.
$KClO_4$	14.7 ± 0.2	n.d.
LiCl	13.1 ± 0.4	0.453 ± 0.04
NaCl	11.4 ± 0.2	0.570 ± 0.01
KCl	15.8 ± 0.2	0.431 ± 0.1
RbCl	12.5 ± 0.3	<0.1
CsCl	9.84 ± 0.2	<0.1

n.d.: not determined

Table S3 Table of the background-subtracted rate constants for ion transport with Star of David catenane **3** and pentafoil knot **2** in a range of salts (20 mM MOPS, 100 mM MX, pH 7.4).

Salt	Star of David catenane **3** ion transport rate (background subtracted) / × 10^{-3} s^{-1}	Pentafoil knot **2** ion transport rate (background subtracted) / × 10^{-3} s^{-1}
KF	3.40 ± 0.1	0.0889 ± 0.1
KCl	15.7 ± 0.2	0.365 ± 0.04
KBr	23.0 ± 0.5	0.405 ± 0.2
KI	30.2 ± 0.2	0.713 ± 0.03
KSCN	31.4 ± 0.5	n.d.
KNO_3	6.57 ± 0.4	n.d.
$KClO_4$	9.77 ± 0.2	n.d.
LiCl	13.0 ± 0.4	0.365 ± 0.04
NaCl	11.2 ± 0.2	<0.1
KCl	15.7 ± 0.2	<0.1
RbCl	12.1 ± 0.3	0.0889 ± 0.01
CsCl	9.84 ± 0.2	0.365 ± 0.01

n.d.: not determined

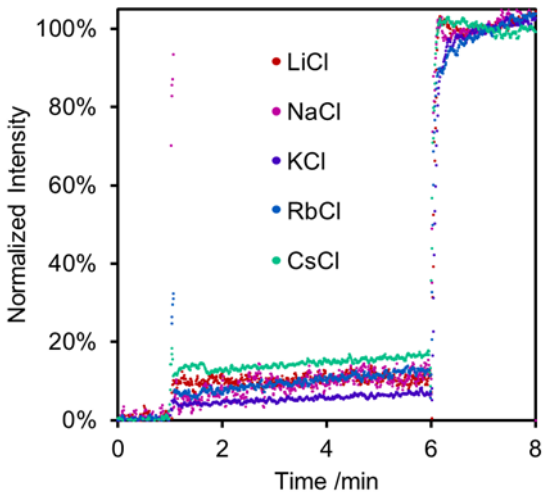

Figure S10 HPTS assays and data fitting for helicate **5** (5 μL of a 1 mM solution) showing the lack of ion transport in a range of salts (20 mM MOPS, 100 mM MX, pH 7.4). Ionophore added at 0 min, base pulse added at 1 min, Triton X-100 added at 6 mins.

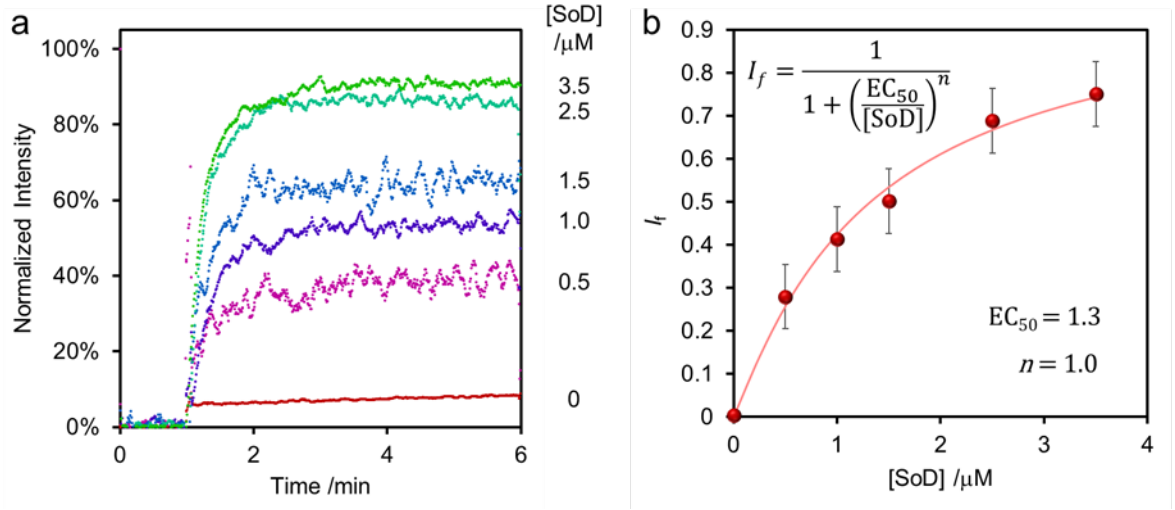

Figure S11 (a) Varying the concentration of Star of David catenane **3** in HPTS assays. Ionophore added at 0 min, base pulse added at 1 min, Triton X-100 added at 6 mins. B The data were fitted to determine the normalized fluorescence ratio at 6 minutes, whereby the absorbance with 0 μM Star of David catenane **3** (approximately 10%) was set as 0 and the maximum absorbance possible was approximated as 100%. The normalized fluorescence values at 6 minutes were thus determined to give I_f fractional absorbance intensity. (b) This was subsequently fitted to the Hill equation[S5] to determine EC_{50} (concentration required for 50% activity as 1.3 ± 0.4 μM) and n (stoichiometry of channel formation as 1.0 ± 0.3).

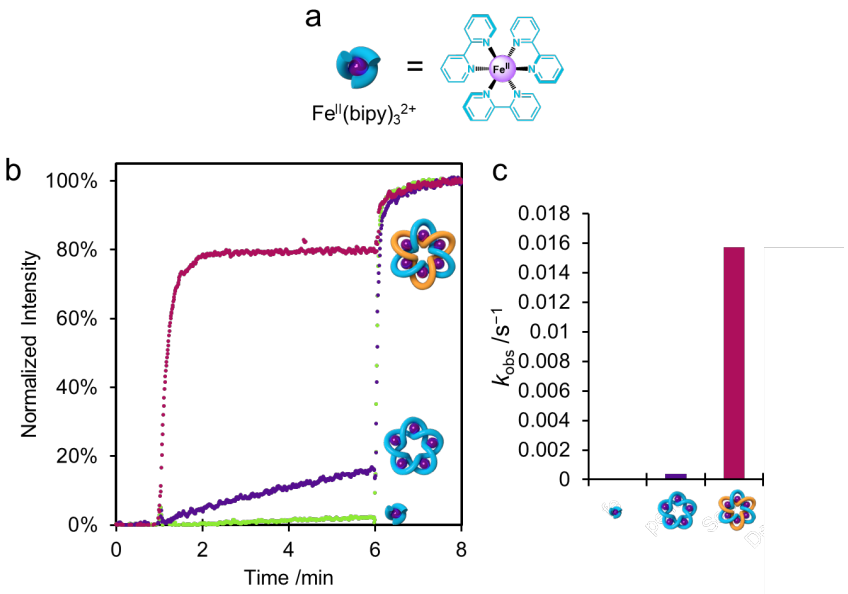

Figure S12 (a) Structure and representation of $Fe^{II}(bipy)_3^{2+}$ complex, (b) HPTS assays and data fitting comparing the rate of ion transport of pentafoil knot **2**, Star of David **3** and $Fe^{II}(bipy)_3^{2+}$ complex (5 μL of a 1 mM solution, 20 mM MOPS, 100 mM KBr, pH 7.4). (c) Observed rate constants for ion transport with background rate subtracted. Ionophore added at 0 min, base pulse added at 1 min, Triton X-100 added at 6 mins.

In situ addition of M^{2+} to Star of David 4

We attempted to complex the demetallated Star of David **4** with zinc(II) *in situ* and thus switch on ion transport in HPTS assays. Remetallation of **4** with iron(II) directly had previously been shown to be unsuccessful.[S6] Briefly, the standard HPTS assay was conducted as previously described with demetallated Star of David **4**. No ion transport was observed. After 4 minutes, a solution of $Zn(BF_4)_2$ in MeCN (60 eq. relative to **4**, 10 eq. per iron binding site) was added. No change in ion transport was observed. We believe the lack of solubility of demetallated link **4** in the buffered solution and the low partitioning constant of Zn(II) in the membrane prevents *in situ* metallation, which is a reaction generally conducted in MeCN.[S6]

The reverse process, *in situ* demetallation of iron-complexed Star of David **3**, was also not possible as the harsh conditions (refluxing NaOH or KCN)[S2] were incompatible with the HPTS assay.

S3.2 Lucigenin assays

Preparation of large unilamellar vesicles for lucigenin assays

Egg yolk phosphatidylcholine (EYPC, 49 mg, 64 μmol) and cholesterol (6 mg, 16 μmol) were dissolved in 2 mL chloroform (spectroscopic grade) in a 10 mL round-bottom flask. Solvent was removed under reduced pressure, resulting in a thin film of lipid on the inside wall of the round-bottom flask, which was dried further under high vacuum for 16 hours. Lucigenin (1 mM) was dissolved in buffer (20 mM 3-(*N*-morpholino) propanesulfonic acid (MOPS), 200 mM $NaNO_3$ adjusted to pH 7.4 using NaOH). The lucigenin buffer solution (1.2 mL) was added to the lipid film. The mixture was subjected to vortex mixing until the film had completely detached from the sides of the flask. The resulting lipid suspension was gently warmed and extruded 19 times through a 200 nm polycarbonate membrane in an Avestin Liposofast extruder to give a suspension of 200 nm large unilamellar vesicles.

Unencapsulated lucigenin dye was removed by gel permeation chromatography (GPC) on PD-10 SEC columns (Sephadex G-25). An aliquot of the vesicle suspension (1 mL) was added to a column that had been equilibrated with the appropriate buffer (the same buffer as used for vesicle preparation, but without added lucigenin). Once the vesicle solution had run onto the GPC column, further buffer (1.5 mL) was added and allowed to run onto the GPC column. A further solution of buffer (3.5 mL) was added to elute the vesicles, which were collected to give a vesicle stock solution (3.5 mL, final concentration of phospholipid = 15.2 mM, final concentration of cholesterol = 3.8 mM). Two coloured bands were visible on the column, indicating successful separation of the lucigenin-loaded vesicles (faster band) from unencapsulated lucigenin (slower band).

Procedure for lucigenin assays

Lucigenin assays and fluorescence normalisation were performed by a modification of published methods.[S7] An aliquot of the vesicle stock solution (100 μL) was diluted with buffer (1.9 mL, the same buffer as used for vesicle preparation but without the added lucigenin – 20 mM MOPS, 200 mM $NaNO_3$, pH 7.4) to give a final volume of 2 mL (final EYPC/cholesterol concentration 0.95 mM). The vesicle suspension was added to a fluorescence cuvette equipped with a stirrer bar. The ionophoric compound (5 μL of a 1 mM solution in MeCN) was added at time 0 mins and the fluorescence emission at 505 nm was observed, resulting from the excitation at 455 nm. A pulse of 480 mM NaCl (aq.) (100 μL) was added after 1 minute. Finally, Triton X-100 detergent in MOPS buffer (20 μL, 10% *v*/*v* solution) was added after 6 minutes to lyse the vesicles. Data were collected for a further 2 minutes to ensure the vesicles were completely lysed.

Data processing and data fitting for lucigenin assays

Data from time courses were normalized from 0% to 100% according to **equation S1** (see **Section S3.1**), with 100% corresponding to the fluorescence ratio prior to NaCl pulse addition, and 0% corresponding to the fluorescence after addition of Triton X-100 and complete lysing of the vesicles. Data were fitted to **equation S2** as for the HPTS assays (**Section S3.1**).

Experimental data for lucigenin assays

A fluorescence change in the lucigenin assay (**Figure S10**) indicated good transport of chloride anions, confirming the transport of anions by the ionophoric compounds.

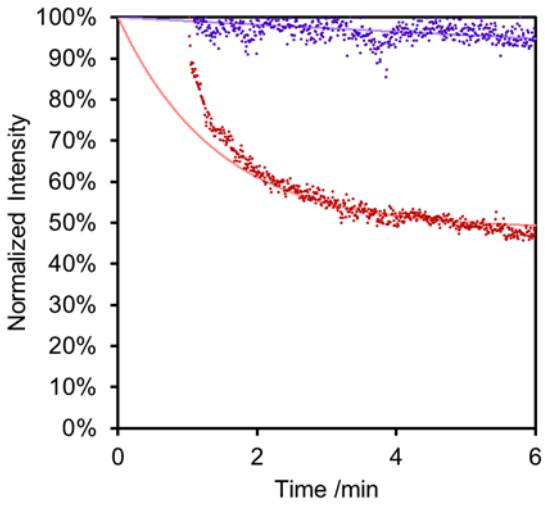

Figure S13 Normalized fluorescence data for lucigenin assays and data fitting for Cl^- transport by MeCN blank (blue, curve fit shown for $k_{obs} = 2.95 \times 10^{-4}$ s^{-1}) and Star of David catenane **3** (red, [**3**] = 2.5 μM, curve fit shown for $k_{obs} = 1.18 \times 10^{-2}$ s^{-1}). Compound added at t = 0 min, 23 mM NaCl added to vesicle exterior at t = 1 min, Triton X-100 added at t = 6 min. (20 mM MOPS, 200 mM $NaNO_3$).

S3.3 CF assays

Preparation of large unilamellar vesicles for CF assays

Egg yolk phosphatidylcholine (EYPC, 49 mg, 64 μmol) and cholesterol (6 mg, 16 μmol) were dissolved in 2 mL chloroform (spectroscopic grade) in a 10 mL round-bottom flask. Solvent was removed under reduced pressure, resulting in a thin film of lipid on the inside wall of the round-bottom flask, which was dried further under high vacuum for 16 hours. 5(6)-Carboxyfluorescein (CF) (50 mM) was dissolved in buffer (20 mM 3-(*N*-morpholino) propanesulfonic acid (MOPS), 100 mM KCl). The buffer pH was raised to pH 11 (by addition of 1 M NaOH) and then acidified to pH 7.4 (by addition of 1 M HCl) to ensure complete dissolution of the CF. The CF buffer solution (1.2 mL) was added to the lipid film. The mixture was subjected to vortex mixing until the film had completely detached from the sides of the flask. The resulting lipid suspension was gently warmed and extruded 19 times through a 200 nm polycarbonate membrane in an Avestin Liposofast extruder to give a suspension of 200 nm large unilamellar vesicles.

Unencapsulated CF dye was removed by gel permeation chromatography (GPC) on PD-10 SEC columns (Sephadex G-25). An aliquot of the vesicle suspension (1 mL) was added to a column that had been equilibrated with the appropriate buffer (the same buffer as used for vesicle preparation, but without added CF). Once the vesicle solution had run onto the GPC column, further buffer (1.5 mL) was added and allowed to run onto the GPC column. A further solution of buffer (3.5 mL) was added to elute the vesicles, which were collected to give a vesicle stock solution (3.5 mL, final concentration of phospholipid = 15.2 mM, final concentration of cholesterol = 3.8 mM). Two orange bands were visible on the column, indicating successful separation of the CF-loaded vesicles (faster band) from unencapsulated CF (slower band).

Procedure for CF assays

The vesicle stock solution (100 μL) was diluted with buffer (1.9 mL, same buffer as used for vesicle preparation but without added CF – 20 mM MOPS, 100 mM KCl, pH 7.4) to give a final volume of 2 mL (final EYPC/cholesterol concentration 0.95 mM). The vesicle suspension was added to a fluorescence cuvette equipped with a stirrer bar. The increase in fluorescence emission at 517 nm was observed (excitation at 492 nm) due to the relief of self-quenching was measured. After 1 minute, the ionophoric compound (5 μL of a 1 mM solution in MeCN) was added, and the fluorescence emission observed. Finally, Triton X-100 detergent in MOPS buffer (20 μL, 10% *v*/*v* solution) was added after 6 minutes to lyse the vesicles. Data were collected for a further 2 minutes to ensure the vesicles were completely lysed.

Data processing for CF assays

Data from time courses were normalized from 0% to 100% according to equation S1 (see **Section S3.1**), with 0% corresponding to the fluorescence ratio prior to ionophoric compound addition, and 100% corresponding to the fluorescence after addition of Triton X-100 and complete lysing of the vesicles.

Experimental data for CF assays

No increase in fluorescence was observed upon addition of the ionophoric compounds to the vesicles (**Figure S11**, 1 minute), indicating that pores large enough to allow escape of the CF dye were not formed by compounds **2** and **3**. By contrast, addition of Triton X-100 (6 minutes) lysed the vesicles and allowed dye release.

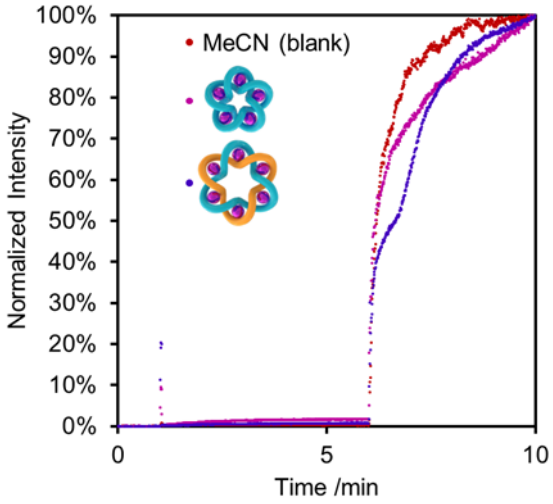

Figure S14 CF assays and data fitting for MeCN blanks, pentafoil knot **2** and Star of David catenane **3** showing the rate of CF efflux from the vesicles (20 mM MOPS, 200 mM $NaNO_3$, pH 7.4). Ionophore added at 1 min, Triton X-100 added at 6 mins.

S3.4 U-tube experiments

Metal picrate U-tube experiments

The procedure used was a modification of published methods.[S8] A solution of chloroform saturated with pentafoil knot **2** or Star of David **3** (approx. 7.5 nM, 10 mL) was added to a glass U-tube (20 mm internal diameter). To the left side of the U-tube was added a sodium picrate solution (2.5 mL, [picrate] = 436 µM, 20 mM MOPS, 100 mM NaCl, pH 7.4) and to the right side was added MOPS buffer (2.5 mL, 20 mM MOPS, 100 mM NaCl, pH 7.4) as a receiving phase. The U-tube was incubated in a water bath at 25 °C and the chloroform phase was stirred at 300 rpm during the entire experiment, ensuring efficient diffusion of any potential carrier-ion complex to the receiving phase (**Figure S13**). Aliquots (1 mL) were taken from the receiving phase and analysed for the presence of picrate by UV spectroscopy (at 356 nm). After measurement, the aliquot was immediately placed back in the U-tube. Measurements were then taken at 0 h, 1 h, 2 h and 24 h. No transport was observed for Star of David catenane **3** (**Figure S14**). A control experiment employed dibenzo-18-crown-6 (1 mM) as a carrier.

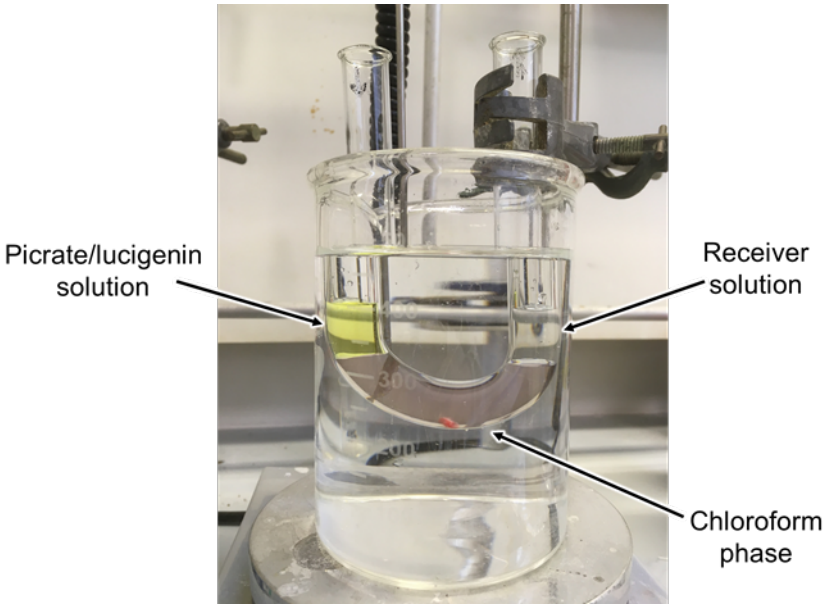

Figure S15 Photograph documenting the U-tube experimental set-up. The dye (picrate or lucigenin, picrate shown in image) was added to the left, and the receiving phase was on the right. The chloroform solution saturated with Star of David catenane **3** (pictured) or pentafoil knot **2** and stirred at 25 °C.

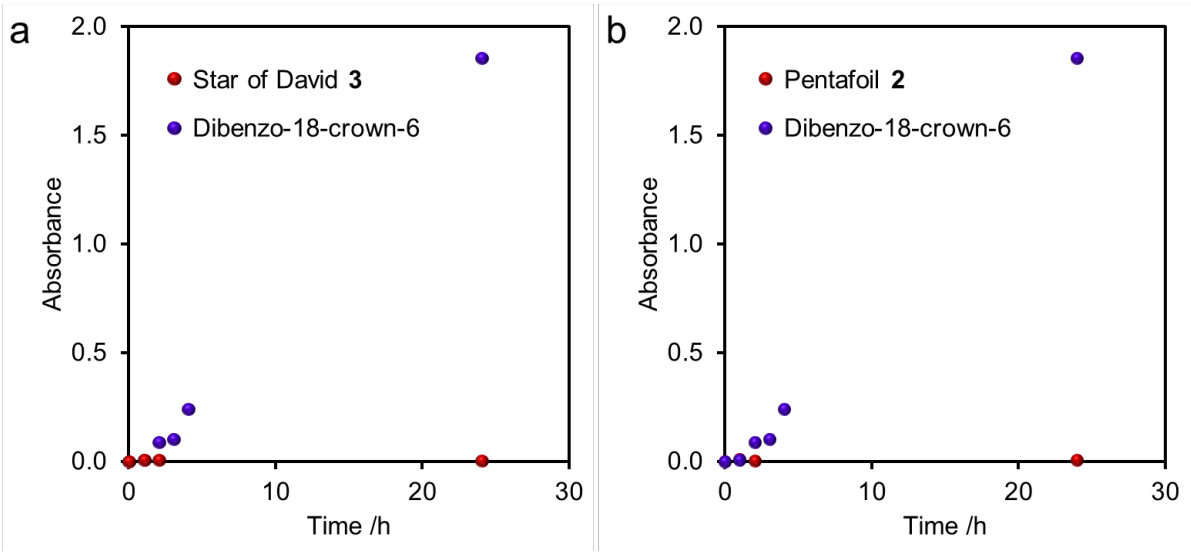

Figure S16 Metal picrate U-tube experiments showing no carrier activity of (a) Star of David catenane **3** or (b) pentafoil knot **2** (red, saturated solution in $CHCl_3$, approx. 7.5 nM) compared to dibenzo-18-crown-6 (blue, 1 mM in $CHCl_3$) employed as a control) (20 mM MOPS, 100 mM NaCl, pH 7.4).

Lucigenin U-tube experiments

The procedure was as above for the metal picrate U-tube experiments, however the left hand side of the tube this time contained a lucigenin solution (2.5 mL, [lucigenin] = 500 µM, 20 mM MOPS, 100 mM NaCl, pH 7.4). The experiment was otherwise conducted as above, with UV measurements conducted at 455 nm to analyse for presence of lucigenin in the receiving phase. No transport was observed for Star of David catenane **3** (**Figure S15**). A control experiment employed 2-aminopentane (1 mM) as a carrier.

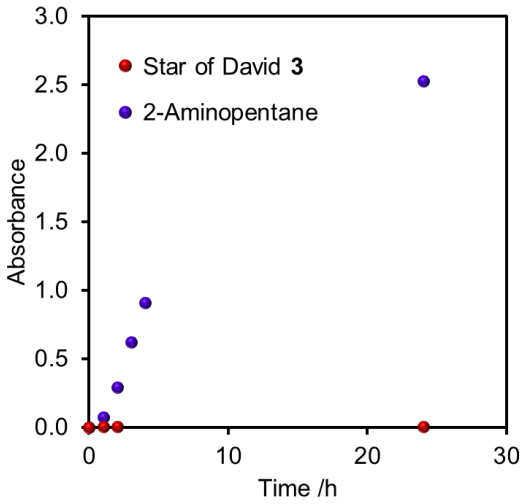

Figure S17 Metal picrate U-tube experiments showing no carrier activity of Star of David catenane **3** (red, saturated solution in $CHCl_3$, approx. 7.5 nM) compared to 2-aminopentante (blue, 1 mM in $CHCl_3$) employed as a control) (20 mM MOPS, 100 mM NaCl, pH 7.4).

S4. Planar bilayer conductance studies

S4.1 Single-channel recordings

Single channel experiments were performed in a custom-built cell. The cell (**Figure S1**) was formed of two Teflon blocks, each with a machine-drilled well (approx. 10 mm diameter and 1 mL volume). Each well contained a side opening, such that when the blocks were bolted together the adjacent side openings connected the two wells. Additionally, each well contained two access channels (approx. 2 mm diameter), drilled at a 45° angle, such that the channels joined the bottom of the main well. An aperture (approx. 100 µm diameter) was created in a Teflon sheet (Goodfellow, 25 µm thick) using a 30kV spark gap generator (Ealing Spark Source). The Teflon sheet containing the aperture was clamped and sealed with silicone glue (3140 RTV coating, Dow Corning) between the two blocks, such that the aperture was positioned in the central lower half of the side opening between the wells.

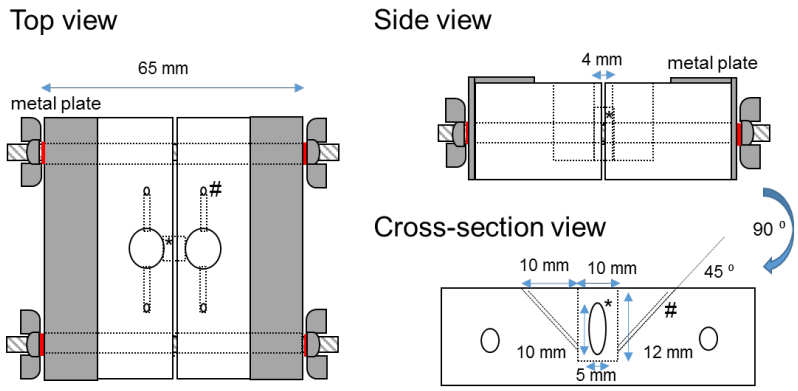

Figure S18 Schematic representation of the cell used in all single channel experiments.

A hanging drop of hexadecane in *n*-pentane (5 mL, 10%, *v*/*v*) was touched on each side of the Teflon sheet and allowed to dry for 1 minute. Buffer (100 mM MOPS or phosphate, 1 M KCl or NaCl, pH 7.4) (600 mL) was added to the well each side of the aperture. EYPC lipid/cholesterol (4:1, *w*/*w*) solution or 1,2-diphytanoyl-*sn*-glycero-3-phosphocholine in *n*-pentane (approx. 10 µL, 10 mg mL^{-1}) was added to each side of the well, and left for approx. 5 mins to allow the pentane to evaporate.

The cell was subsequently placed into a Faraday cage and Ag/AgCl electrodes (Warner), connected to a patch clamp amplifier (Axopatch 200B, Molecular Devices), were suspended either side of the Teflon sheet. The buffer solution on both sides of the Teflon sheet was aspirated and dispensed using a Hamilton syringe to 'paint' a phospholipid bilayer across the aperture. A ± 1 mV pulse was applied at 1333 Hz to determine when a bilayer was obtained (capacitance of 40 to 80 pF). The membrane was characterized with successive 2 second sweeps under an applied potential ranging from +100 to −100 mV (0 → +100 → 0 → −100 → 0 mV). The membrane was deemed acceptable if the range of current flow across the membrane measured < 1 pA in > 10 consecutive characterization sweeps.

The appropriate compound (10 μL of a 1 mM solution in MeCN) was added to the ground well resulting in a final concentration of 8 μM. Characterization sweeps (0 → +100 → 0 → −100 → 0 mV) were continued for 2 hours, or until substantial channel-forming activity was observed.

All data were collected using the patch clamp amplifier, and digitised (Axon Instruments Digidata 1332A) at a sample rate of 50 kHz with a 2 kHz Lowpass Bessel Filter. Single-channel ion current recordings were processed with Clampex 10.2 and Clampfit 10.2 software, where baseline correction was applied and the data were filtered with a 200 Hz −3 dB cut-off.

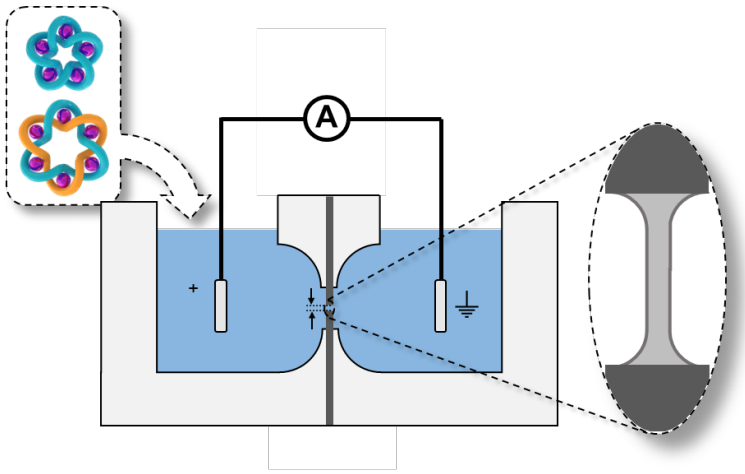

Figure S19 Cartoon showing the experimental procedure for planar bilayer measurements. A potential was applied at the live electrode (right) and the ionophore was added to the ground well (left).

S4.2 Representative single-channel current traces

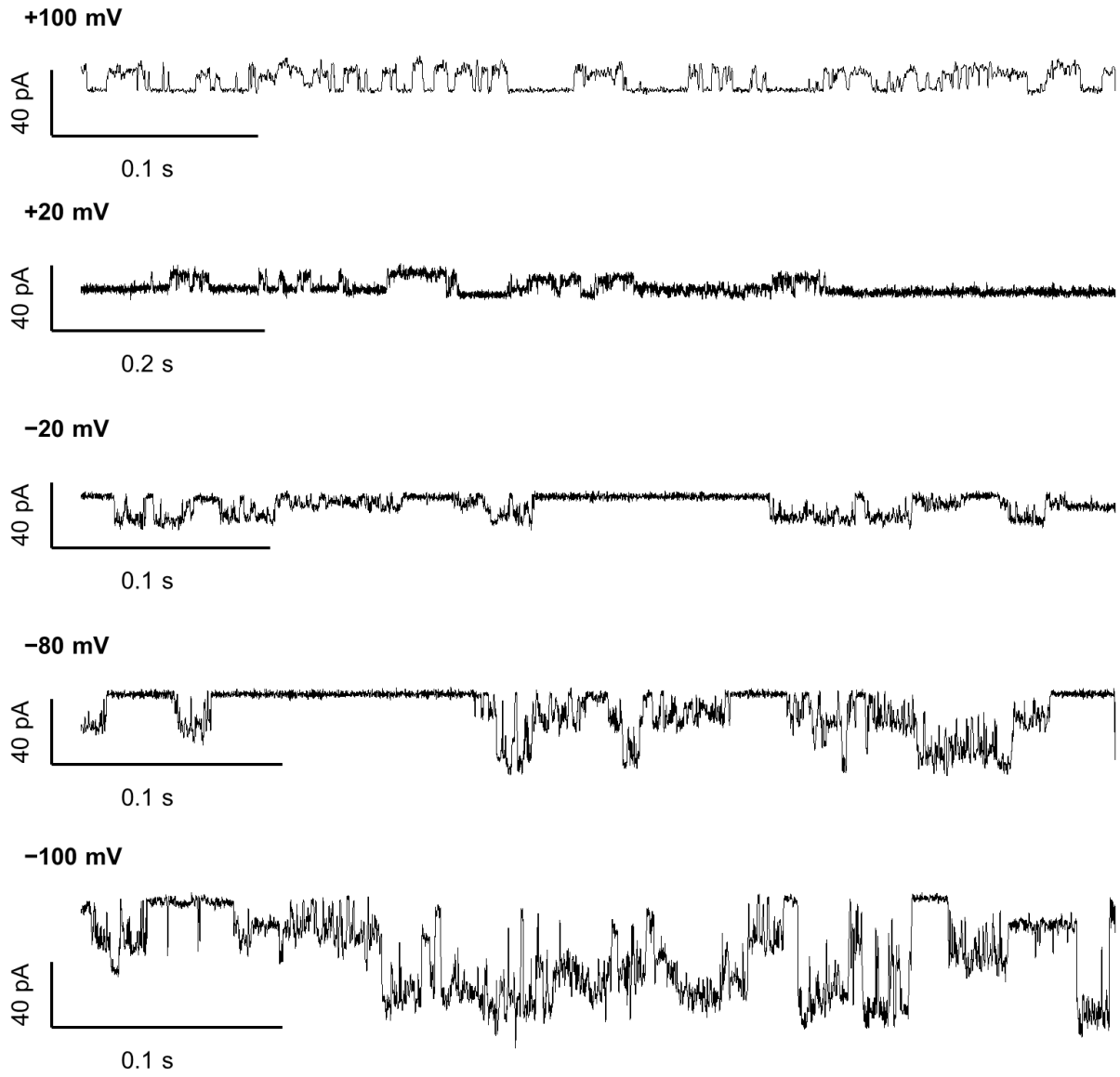

Figure S20 Representative single-channel planar bilayer current traces of ion channel formation with Star of David catenane **3** (EYPC lipid/cholesterol (4:1, w/w), [**3**] = 8 mM, 1 M KCl, 20 mM MOPS, pH 7.4, 293 K) at a range of different voltages

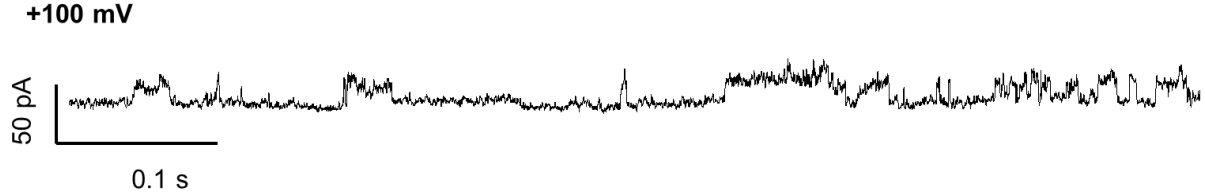

Figure S21 Representative single-channel planar bilayer current traces of ion channel formation with Star of David catenane **3** (1,2-diphytanoyl-*sn*-glycero-3-phosphocholine lipid, [**3**] = 8 mM, 1 M KCl, 20 mM MOPS, pH 7.4, 293 K) at a +100 mV.

S4.3 All-points analysis

Histograms of the measured ion currents were plotted from single-channel data as seen in **Figure 3B**. Current histograms of the current traces were plotted with a bin width of 0.01 pA. The raw data (with no additional digital filtering) was used for this analysis.

Subsequently, the histograms were fitted to two Gaussian distributions according to **equation S3**:

$$f(x) = \left(a_1 e^{-\frac{(x-b_1)^2}{2{c_1}^2}}\right) + \left(a_2 e^{-\frac{(x-b_2)^2}{2{c_2}^2}}\right) \qquad \textbf{equation S3}$$

Where *b* defines the centre of the gaussian distribution while *a* and *c* define its height and width respectively. Values for *a*, *b* and *c* were fitted iteratively using the solver function in Microsoft Excel 2016, minimising the square of the residuals between the data and the fitted model using an iterative method. The difference between the centres of the histograms corresponded to the current of a single channel at the applied voltage (+100 mV in the case of data analysed in **Figure 3B**).

The conductance *G* of a single channel could thus be calculated using **equation S4**:

$$G = \frac{I}{V} \qquad \textbf{equation S4}$$

Where *I* is the current and *V* is the applied voltage.

S4.4 Estimation of channel diameter

We have used the Hille equation[S9] to estimate the pore sizes that correspond to the different conductance levels observed. A correction based on fitting a flexible pore with variable dimensions to Hille's simplified model, Sansom's correction factor of (c) = 4.9 was applied to the measured conductances.[S10]

The corrected values (g) were applied in the Hille **equation S5**:

$$(g)^{-1} = \frac{4l\rho}{\pi d^2} + \frac{\rho}{d} \qquad \textbf{equation S5}$$

Two different channel lengths were considered. The first was the approximate width of an EYPC bilayer[S11] (l = 3.4 nm), whilst the second was the approximate thickness of the Star of David catenane **3** (l = 1.55 nm, Figure 4 in the main text).The latter value may be a more appropriate value if membrane thinning is occurring. The solution resistivity was ρ = 9.44 Ω·m (for 1 M KCl).[S12,S13] These calculations provide approximate pore diameters of 7.2 Å or 5.0 Å for each respective estimated pore length.

Table S4 Corrected Hille calculation for Star of David **3**.

Conditions	Conductance	Channel Length	Estimated diameter
+100 mV in KCl	0.22 ± 0.7 nS	3.4 nm (bilayer width)	7.2 ± 1.3 Å
+100 mV in KCl	0.22 ± 0.7 nS	1.55 nm (SoD thickness)	5.0 ± 1.0 Å

.

S5. References

S1 Marcos, V.; Stephens, A. J.; Jaramillo-Garcia, J.; Nussbaumer, A. L.; Woltering, S. L.; Valero, A.; Lemonnier, J.-F.; Vitorica-Yrezabal, I. J.; Leigh, D. A. Allosteric initiation and regulation of catalysis with a molecular knot. *Science* **2016**, *352*, 1555–1559.

S2 Leigh, D. A.; Pritchard R. G.; Stephens, A. J. A Star of David Catenane *Nat. Chem.* **2014**, *6*, 978–982.

S3 Hasenknopf, B.; Lehn, J.-M.; Boumediene, N.; Dupont-Gervais, A.; Van Dorsselaer, A.; Kneisel, B.; Fenske, D. Self-Assembly of Tetra- and Hexanuclear Circular Helicates. *J. Am. Chem. Soc.* **1997**, *119*, 10956–10962.

S4 Gorteau, V.; Bollot, G.; Mareda, J.; Matile, S. Rigid-rod anion–π slides for multiion hopping across lipid bilayers. *Org. Biomol. Chem*. **2007**, *5*, 3000–3012.

S5 Yifrach, O. Hill coefficient for estimating the magnitude of cooperativity in gating transitions of voltage-dependent ion channels. *Biophys. J.* **2004**, *87*, 822–830.

S6 Zhang, L.; Stephens, A. J.; Lemonnier, J.-F.; Pirvu, L.; Vitorica-Yrezabal, I. J.; Robinson C. J.; Leigh, D. A. Coordination chemistry of a molecular pentafoil knot. *J. Am. Chem. Soc.* **2019**, *141*, 3952–3958.

S7 Seganish, J. L.; Fettinger, J. C.; Davis, J. T. Facilitated chloride transport across phosphatidylcholine bilayers by an acyclic calixarene derivative: Structure-function relationships *Supramol. Chem.*, **2006**, *18*, 257–264.

S8 Jones, J. E.; Diemer, V.; Adam, C.; Raftery, J.; Ruscoe, R. E.; Sengel, J. T.; Wallace, M. I.; Bader, A.; Cockroft, S. L.; Clayden, J.; Webb, S. J. Length-dependent formation of transmembrane pores by 3_{10}-helical alpha-aminoisobutyric acid foldamers. *J. Am. Chem. Soc.* **2016**, *138*, 688−695.

S9 Hille, B. *Ionic Channels of Excitable Membranes*; 3rd Edition, Sinauer, Sunderland, MA, 2001.

S10 Smart, O.S.; Breed, J.; Smith, G.R.; Sansom, M.S. A novel method for structure-based prediction of ion channel conductance properties. *Biophys. J.* **1997**, *72*, 1109−1126.

S11 Sakai, N.; Kamikawa, Y.; Nishii, M.; Matsuoka, T.; Kato, T. Matile, S. Dendritic Folate Rosettes as Ion Channels in Lipid Bilayers, *J. Am. Chem. Soc.* **2006**, *128*, 2218−2219.

S12 Malla, J. A.; Umesh, R. M.; Vijay, A.; Mukherjee, A.; Lahiri, M.; Talukdar, P. Apoptosis-inducing activity of a fluorescent barrel-rosette M^+/Cl^- channel. *Chem. Sci.* **2020**, *11*, 2420−2428.

S13 Vanýsek, P. in *CRC Handbook of Chemistry and Physics*, 91st edition; Haynes, W. M. 2010; pp. 5−74.